MOLECULAR AND CELLULAR BIOLOGY, Oct. 2011, p. 4076–4086 Vol. 31, No. 19
0270-7306/11/$12.00 doi:10.1128/MCB.05152-11

Antagonistic Regulation of Cystic Fibrosis Transmembrane Conductance Regulator Cell Surface Expression by Protein Kinases WNK4 and Spleen Tyrosine Kinase[▽]

Ana Isabel Mendes,[1,3] Paulo Matos,[1,3] Sónia Moniz,[1,3] Simão Luz,[2,3] Margarida D. Amaral,[2,3] Carlos M. Farinha,[2,3] and Peter Jordan[1,3]*

Department of Genetics, National Health Institute Dr. Ricardo Jorge, Lisbon, Portugal[1]; Department of Chemistry and Biochemistry, Faculty of Sciences, University of Lisbon, Lisbon, Portugal[2]; and BioFIG-Center for Biodiversity, Functional and Integrative Genomics, University of Lisbon, Lisbon, Portugal[3]

Received 1 February 2011/Returned for modification 11 March 2011/Accepted 22 July 2011

Members of the WNK (with-no-lysine [K]) subfamily of protein kinases regulate various ion channels involved in sodium, potassium, and chloride homeostasis by either inducing their phosphorylation or regulating the number of channel proteins expressed at the cell surface. Here, we describe findings demonstrating that the cell surface expression of the cystic fibrosis transmembrane conductance regulator (CFTR) is also regulated by WNK4 in mammalian cells. This effect of WNK4 is independent of the presence of kinase and involves interaction with and inhibition of spleen tyrosine kinase (Syk), which phosphorylates Tyr512 in the first nucleotide-binding domain 1 (NBD1) of CFTR. Transfection of catalytically active Syk into CFTR-expressing baby hamster kidney cells reduces the cell surface expression of CFTR, whereas that of WNK4 promotes it. This is shown by biotinylation of cell surface proteins, immunofluorescence microscopy, and functional efflux assays. Mutation of Tyr512 to either glutamic acid or phenylalanine is sufficient to alter CFTR surface levels. In human airway epithelial cells, downregulation of endogenous Syk and WNK4 confirms their roles as physiologic regulators of CFTR surface expression. Together, our results show that Tyr512 phosphorylation is a novel signal regulating the prevalence of CFTR at the cell surface and that WNK4 and Syk perform an antagonistic role in this process.

Ion transport across the plasma membrane is regulated by posttranslational mechanisms that rapidly modify the amount of ion channel proteins present at the plasma membrane and/or their transport activity, processes requiring tight regulation by signaling mechanisms.

One novel signaling pathway in the kidney that involves members of the WNK (with-no-lysine [K]) protein kinase family of serine/threonine protein kinases was recently identified (43). It was found that mutations in the *WNK1* and *WNK4* genes result in increased renal sodium (Na^+) and chloride (Cl^-) reabsorption and impaired potassium (K^+) secretion, manifesting as the inherited syndrome of hypertension and hyperkalemia, also known as pseudohypoaldosteronism type II (PHA2) or Gordon's syndrome (45). Affected patients carry missense mutations in *WNK4* that, when expressed in cell models, have been shown to lead to the deregulation of the renal Na^+/Cl^- cotransporter (NCC) and renal outer medullary potassium channel 1 (ROMK1) (13, 21, 32, 46). Results of analysis of transgenic mouse models of the disease suggest that changes in both the surface expression and the activity of NCC are the main pathological mechanisms underlying PHA2 (23, 30, 50).

The ion transport activity of the NCC, as well as of the related $Na^+/K^+/Cl^-$ cotransporter 1 (NKCC1) and NKCC2 channels, is regulated by phosphorylation on N-terminal threonine residues by one of two STE20-family protein kinases, Ste20-related proline and alanine-rich kinase (SPAK) or oxidative stress-responsive kinase 1 (OSR1) (20, 31, 33). Both kinases require activation by WNK4, which phosphorylates residue Thr233 in SPAK or Thr185 in OSR1 (12, 28, 44).

WNK4 can further regulate the surface amount of other renal or extrarenal ion channels in a kinase-independent manner when expressed in *Xenopus* oocytes or mammalian cells. These include NCC (5, 14, 37, 46, 47, 49, 52), the $Cl^-/HCO3^-$ exchangers SLC26A6 (19) and SLC16A9 (8), ROMK1 (22, 29, 35), the epithelial Na^+ channel (ENaC) (16, 34), transient receptor potential vanilloid calcium channel 4 (TRPV4) (10) and TRPV5 (7, 18), and the cystic fibrosis (CF) transmembrane conductance regulator (CFTR) Cl^- channel (48), mutation of which is the cause of CF.

In the case of ROMK and TRPV5, mutant WNK4 was shown to interact with the scaffold protein Intersectin and promote channel endocytosis (7, 15, 22), but whether other mechanisms exist through which WNK4 regulates ion channel surface expression remains unknown. The elucidation of such mechanisms may help to identify drug targets to correct the insufficient channel activity that underlies several diseases (6, 17). For example, in CF patients, the lack of CFTR activity leads to dehydrated, thick mucus in the lungs and subsequent chronic bacterial infections; however, disease symptoms would be sig-

* Corresponding author. Mailing address: Departamento de Genética, Instituto Nacional de Saúde Dr. Ricardo Jorge, Avenida Padre Cruz, 1649-016 Lisbon, Portugal. Phone: 351-21-7519380. Fax: 351-21-7526410. E-mail: peter.jordan@insa.min-saude.pt.

▽ Published ahead of print on 1 August 2011.

nificantly reduced if only about 10% of CFTR activity could be restored in patients (2).

Here we identified a novel signaling mechanism linking the cell surface expression of CFTR to protein kinase WNK4 and the spleen tyrosine kinase (Syk). Syk is a cytoplasmic nonreceptor tyrosine kinase best known for its proinflammatory role in immunoreceptor signaling in leukocytes (27). We show in this work that Syk can phosphorylate CFTR and decrease surface CFTR expression and that the interaction of WNK4 with Syk prevents CFTR phosphorylation and promotes an increase in CFTR-mediated ion transport.

MATERIALS AND METHODS

Cell culture and transfections. HEK293 (human embryonic kidney) cells were maintained in Dulbecco's minimal essential medium (DMEM) supplemented with 10 U of penicillin/ml, 10 μg of streptomycin/ml, and 10% fetal calf serum (Invitrogen S.A., Barcelona, Spain) and were regularly checked for the absence of mycoplasm infection. Baby hamster kidney (BHK-21) cells stably expressing human wild-type (wt) CFTR (BHK-21-CFTR) (26, 38) were maintained in DMEM-F12 medium supplemented with L-glutamine, 15 mM HEPES, 10 U of penicillin/ml, 10 μg of streptomycin/ml, 0.2% methotrexate, and 5% fetal calf serum (Invitrogen). The CF patient-derived human bronchial epithelial cell line CFBE41o-, stably expressing wild-type CFTR (3) (generous gift from J. P. Clancy, University of Alabama at Birmingham), was grown at 37°C under conditions of 5% CO_2, in minimal essential medium (MEM) supplemented with L-glutamine, 10% FBS, and penicillin-streptomycin (all from Invitrogen, Spain). The cells were routinely grown on plastic flasks coated with fibronectin-vitrogen-bovine serum albumin (fibronectin-vitrogen-BSA) as previously described (3). All cell lines were regularly checked for absence of mycoplasm infection.

For ectopic expression of plasmid cDNAs, HEK293 cells were transfected at 80 to 90% confluence using Metafectene (Biontex, Martinsried/Planegg, Germany) according to the manufacturer's instructions. BHK-21 cells were transfected at 80 to 90% confluence using Lipofectamine 2000 (Invitrogen) according to the manufacturer's instructions. Transfection efficiencies were found to be around 90%, as determined microscopically using a green fluorescent protein (GFP) expression vector. The amount of transfected plasmid DNA was kept constant at 4 μg per 60-mm-diameter dish or 2 μg per 35-mm-diameter dish; constructs were supplemented with empty vector if required. For immunofluorescence studies, constructs were diluted 1:4 with empty pcDNA3 vector to reduce transfection efficiency and allow imaging of transfected and nontransfected cells side by side. All transfected cells were analyzed after 20 h for biochemical assays or after 16 h for immunofluorescence experiments. For downregulation of endogenous proteins, 300 pmol of the corresponding specific small interfering RNAs (siRNAs), namely, sc-29501 (from Santa Cruz Biotechnologies) against Syk and NM_032387si5 (5′ACA CUA CAG ACA CUA CAG A) (from Eurofins MWG Operon, Ebersberg, Germany) against WNK4, was transfected into CFBE41o- cells by the use of Lipofectamine 2000 (Invitrogen). A luciferase GL2 siRNA (Eurofins MWG Operon) was used as a control, and cells were analyzed 48 h after transfection. All results were confirmed in at least three independent transfection experiments.

Transcript expression analysis. Total RNA was extracted from CFBE cells by the use of an RNeasy kit (Qiagen, Hilden, Germany), and 1 μg of the extracted content was used for reverse transcription (RT) using random primers (Invitrogen) and Ready-to-Go You-Prime beads (GE Healthcare, Buckinghamshire, United Kingdom). The primers for specific amplification of WNK4 were WNK4_ex12F (5′CAG ACG GAT TCG GGA GAT TA) and WNK4_ex14R (5′TGG GTT TCC AGG AGA CAA AG), for Syk were Syk SI-F (5′AGC TGG ACA ACC CGT ACA TC) and Syk SI-R (5′TGT GCA CAA AAT TGC TCT CC), and for RNA polymerase II (POLR2) were pol II-F (5′-GAG CGG GAA TTT GAG CGG ATG C) and pol II-R (5′-GAA GGC GTG GGT TGA TGT GGA AGA). Amplification reactions were performed using AmpliTaq polymerase (Perkin Elmer, Wellesley, MA) and 35 cycles of 94°C for 20 s, 58°C for 20 s, and 72°C for 20 s, with an initial denaturation of 5 min at 94°C and a final extension of 10 min at 72°C for WNK4, 28 cycles of 94°C for 30 s, 58°C for 30 s, and 72°C for 30 s for Syk, or 28 cycles of 94°C for 30 s, 64°C for 30 s, and 72°C for 30 s for POLR2. These amplification conditions were semiquantitative and experimentally determined to correspond to the linear amplification phases. Products were separated on 2% agarose gels, and band intensity was quantified using Image J software followed by POLR2 normalization. No amplification was obtained when RNA was mock reverse transcribed without addition of reverse transcriptase.

Expression constructs. Partial cDNA clones encoding human WNK4 and its kinase-dead mutant K186A (both kindly provided by X. Jeunemaître, Paris, France) were completed by substituting a PCR-amplified 2-kb fragment to generate a complete WNK4 sequence identical to that corresponding to GenBank accession no. NM_032387. The WNK4 cDNAs were then subcloned into either pEGFP (BD Biosciences Europe, Erembodegem, Belgium) or pcDNA3-Myc (Invitrogen) expression vector. The yellow fluorescent protein-Syk (YFP-Syk) vector (whose coding sequence corresponds to that of GenBank NM_001135052) was purchased from RZPD-ImaGenes (Berlin, Germany), and its kinase-dead mutant, YFP-Syk-K402R, was generated by mutating codon 402 from AAA to AGA by the use of a QuikChange mutagenesis kit (Stratagene, La Jolla, CA). pET-Sumo-NBD1 (the first nucleotide binding domain [NBD]of CFTR; kindly provided by Philip J. Thomas, Dallas, TX) was mutated at CFTR codon 512 from TAT to TTT to obtain pET-Sumo-NBD1-Y512F. For subcloning of Myc-tagged NBD1 and NBD1-Y512F, their cDNAs, which correspond to CFTR codons 388 to 677, were amplified from pET-Sumo-NBD1 by the use of primers NBD1-F (5′ ACG ACT ACA GAA GTA GTG ATG) and NBD1-R (5′ TTA GAC AGG AGC ATC TCC TTC), cloned into pCR2.1 Topo-TA vector (Invitrogen), and transferred into a pcDNA3-Myc expression vector. CFTR-Y512F and CFTR-Y512E mutants were generated by changing codon 512 of human pNUT-CFTR (26) from TAT to TTT and GAG, respectively. Protein kinase OSR1 (oxidative stress-responsive kinase 1) was amplified from cDNA clone IRAUp969A0428D (RZPD-ImaGenes, Berlin, Germany) by PCR with primers Bam-OSR1-F (5′ GGA TCC ATG TCC GAG GAC TCG AG) and Hind-OSR1-R (5′ TTC GAA TTA GCT GAT GCT GAG CTG), cloned into pCR2.1 Topo-TA vector, and then subcloned into the BamHI and HindIII sites of T7/His-tagged pET28 vector (Novagen). Subsequently, codon 164 of the cDNA was mutated from GAC to GCC to generate the kinase-dead OSR1-D164A mutant, which was used as a substrate for *in vitro* protein kinase assays. Myc-tagged hnRNP A1 (a gift from H. König, Karlsruhe, Germany) was as described previously (25). All constructs were verified by automated DNA sequencing.

Coimmunoprecipitation and Western blot procedures. For coimmunoprecipitation experiments, cells were grown in 60-mm-diameter dishes (transfected cells) and lysed on ice in 250 μl of nondenaturing lysis buffer (50 mM Tris-HCl [pH 7.5], 1% NP-40, 100 mM NaCl, 10% glycerol, 10 mM $MgCl_2$) supplemented with a protease inhibitor cocktail composed of 1 mM phenylmethylsulfonyl fluoride (PMSF), 1 mM 1,10-phenanthroline, 1 mM EGTA, 10 μM E64, and 10 μg/ml of each aprotinin, leupeptin, and pepstatin A (all from Sigma-Aldrich Quimica, Madrid, Spain). The cell lysates were incubated for 2 h at 4°C with the specified antibodies, namely, anti-GFP ab1218 (Abcam, Cambridge, United Kingdom) (2.5 μg/ml) and anti-Myc clone 9E10 (M5546; Sigma-Aldrich), further incubated for 1 h with protein G-agarose beads (Roche Applied Science, Indianapolis, IN), and finally washed three times in cold lysis buffer containing 200 mM NaCl. Proteins were solubilized from the beads in 2× sodium dodecyl sulfate (SDS) sample buffer and separated in a 10% SDS-polyacrylamide gel electrophoresis (SDS-PAGE) Protean III minigel (Bio-Rad, Hercules, CA). All gels intended for assessment of CFTR expression contained 1% glycerol and were run at 4°C. For detection of specific proteins, the polyacrylamide gel was transferred onto a polyvinylidene difluoride (PVDF) membrane (Bio-Rad) by the use of a Mini Trans-Blot cell (Bio-Rad) (100 V for 1 h) followed by Coomassie staining to check for equal transfer results. Western blot membranes were blocked in Tris-buffered saline (TBS)–0.1% Triton X-100–5% milk powder, probed using the indicated antibodies, and then incubated with a secondary peroxidase-conjugated antibody (Bio-Rad) followed by chemiluminescence detection. Primary antibodies used for Western blot analyses were rabbit anti-Myc A14 (sc-789) from Santa Cruz Biotechnologies (Santa Cruz, CA), rabbit anti-GFP ab290 from Abcam (Cambridge, United Kingdom), mouse anti-T7-tag from Merck4Biosciences (Nottingham, United Kingdom), mouse anti-human transferrin receptor (TfR) (clone H68.4; Invitrogen Corporation, CA), mouse anti-CFTR clone 596 (obtained through the University of North Carolina at Chapel Hill [UNC] CFTR antibody distribution program sponsored by Cystic Fibrosis Foundation Therapeutics, Inc. [CFFT]) to detect full-length CFTR in cell extracts, mouse anti-CFTR clone L12B4 (mAb3484) from Chemicon International (Billerica, MA) to detect recombinant NBD1 (rNBD1), and affinity-purified rabbit anti-CFTR (Lis1) (9) to detect CFTR in immunoprecipitates obtained with mouse anti-GFP.

For protein-protein interaction screening, a signal transduction antibody array from Hypromatrix (Worcester, MA) containing antibodies against 400 cellular proteins involved in signal transduction was used. The array membranes were incubated for 2 h at room temperature with cell lysates prepared in nondenaturing lysis buffer from four 60-mm-diameter dishes of HEK293 cells transfected

with either Myc-WNK4 or empty vector and then washed like Western blots before being subjected to staining of the complexes containing Myc-WNK4 with an anti-Myc peroxidase conjugate (from Hypromatrix).

Biotinylation of cell surface proteins. Cells were transfected as described above, washed twice with warm culture medium to remove dead cells, and placed on ice in a cold room. Cells were washed three times with ice-cold phosphate-buffered saline–CM (PBS-CM) (PBS [pH 8.0] containing 0.1 mM $CaCl_2$ and 1 mM $MgCl_2$) and left for 5 min in cold PBS-CM to ensure arrest of endocytic traffic. Cells were then incubated for 30 min with EZlink sulfo-NHS-SS-biotin (catalog no. 21331; Pierce Biotechnology, Rockford, IL) (0.5 mg/ml) in PBS-CM before being rinsed twice and left for 15 min on ice with ice-cold Tris-glycine (100 mM Tris-HCl [pH 8.0], 150 mM NaCl, 0.1 mM $CaCl_2$, 1 mM $MgCl_2$, 10 mM glycine, 1% BSA) to quench the biotinylation reaction. Cells were again washed 3 times with cold PBS-CM and lysed in 250 μl of pull-down buffer (50 mM Tris-HCl [pH 7.5], 100 mM NaCl, 10% glycerol, 1% NP-40) in the presence of the aforementioned protease inhibitor cocktail. The cell lysates were harvested by scraping and cleared by centrifugation at 16,000 × *g* at 4°C for 5 min. An aliquot of 40 μl representing the total CFTR level was removed and added to 2× CFTR sample buffer (62.5 mM Tris-HCl [pH 6.8], 3% SDS, 10% glycerol, 0.02% bromophenol blue, 160 mM dithiothreitol [DTT]), while 200 μl of lysate was added to 25 μl of streptavidin-agarose beads (Sigma-Aldrich) previously incubated for 1 h in 1 ml of cold pulldown buffer containing 2% nonfat milk powder and washed 3 times in pulldown buffer. For purification of biotinylated proteins, lysates and beads were incubated under conditions of rotation for 1 h at 4°C, and the beads were collected by centrifugation (1 min at 3,000 × *g*) and washed 3 times in cold wash buffer (100 mM Tris-HCl [pH 7.5], 300 mM NaCl, 1% Triton X-100). Captured proteins were recovered from the beads in 25 μl of 2× CFTR sample buffer without boiling. The biotinylated protein fraction and 1/20 of the corresponding whole-cell lysate were analyzed alongside by SDS-PAGE followed by Western blot transfer.

Production of recombinant OSR1 or Sumo-NBD1 and *in vitro* protein kinase assays. For the production of recombinant human OSR1, a reported WNK4 substrate (44), or of recombinant human NBD1 domain, pET-OSR1-D164A, pET-Sumo-NBD1, and pET-Sumo-NBD1-Y512F were expressed in the *Escherichia coli* BL21 strain under conditions of isopropylthiogalactosidase (IPTG) (0.1 mM) induction and the bacterial pellets were harvested by centrifugation at 1,400 × *g* for 20 min and frozen. For protein extraction, pellets were resuspended in either conventional lysis buffer (50 mM Tris-HCl [pH 7.5], 50 mM NaCl, 5 mM $MgCl_2$, 1 mM DTT) for OSR1 or CFTR lysis buffer (50 mM Tris-HCl [pH 7.5], 100 mM L-arginine, 50 mM NaCl, 5 mM $MgCl_2$, 12.5% glycerol, 0.25% NP-40, 0.1% SDS, 1 mM DTT, 2 mM ATP) in the presence of the protease inhibitor cocktail described above and then sonicated (Sonics Vibra Cell sonicator, set at 40% amplitude) on ice for 10 cycles of 30 s with 10-s intervals. Following centrifugation of the extract at 16,000 × *g*, the supernatant was incubated with nickel-nitrilotriacetic acid (Ni-NTA)–agarose beads (Qiagen, Hilden, Germany) for 1 h at 4°C. Beads were washed twice with cold lysis buffer containing 20 mM imidazole and protease inhibitors. Recombinant OSR1 was eluted and stored in cold lysis buffer containing 250 mM imidazole, whereas recombinant Sumo-NBD1 proteins were dialyzed using imidazole-free lysis buffer and then concentrated. Proteins were quantified and stored in aliquots at −80°C.

For *in vitro* protein kinase assays, cells were lysed under stringent conditions in 250 μl of radioimmunoprecipitation (RIPA) buffer (50 mM Tris-HCl [pH 7.5], 1% NP-40, 150 mM NaCl, 0.1% SDS, 0.5% sodium deoxycholate) supplemented with protease inhibitors (see above). To reduce extract viscosity, benzonase (Sigma-Aldrich) (500 U/ml) and 5 mM $MgCl_2$ were added. Following immunoprecipitation of WNK4 or Syk as described above, the resulting beads were washed three times in cold RIPA buffer followed by three washes with nondenaturing lysis buffer and then resuspended in 20 μl of kinase reaction buffer (30 mM Tris HCl [pH 7.5], 10% glycerol, 1 mM DTT, 1 mM Na_3VO_4, 10 mM $MgCl_2$, 2 mM $MnCl_2$, 150 μM ATP), mixed with the corresponding substrate (1,000 ng of recombinant kinase-dead OSR1 or recombinant NBD1 or beads containing immunoprecipitated Myc-tagged NBD1 or full-length CFTR protein), and incubated in the presence of 5 μCi of [γ-^{32}P]ATP at 30°C for 30 min. When immunoprecipitated endogenous CFTR protein was used as the substrate, the *in vitro* phosphorylation reaction was preceded by incubation with unlabeled ATP for 30 min at 30°C to reduce background phosphorylation. In addition, the reaction was performed in the presence of inhibitors of protein serine/threonine kinases known to phosphorylate CFTR *in vitro* (1), namely, 2 μM bisindolylmaleimide II (Sigma-Aldrich) to inhibit protein kinases C and A and 50 μM quinalizarin (1,2,5,8-tetrahydroxyanthraquinone) to inhibit casein kinase II (kind gift from L. Pinna, Padua, Italy). Finally, 2× SDS sample buffer was added and samples were boiled. For full-length CFTR, 2× CFTR sample buffer was added without boiling. Samples were then separated by SDS-PAGE followed by Western blot analysis. PVDF membranes were dried and first exposed to X-ray films for 10 to 72 h and subsequently rehydrated for immunodetection with the indicated antibodies in order to document protein quantities.

Immunofluorescence microscopy. BHK-21 cells were grown on coverslips, transfected as indicated, fixed after 16 h with 4% formaldehyde (catalog no. 104003; Merck Chemicals, Darmstadt Germany)–PBS, and permeabilized with 0.2% Triton X-100–PBS. Cells were then immunolabeled for 1 h with mouse anti-CFTR (clone 570; obtained through the UNC CFTR antibody distribution program sponsored by CFFT), washed 3 times for 5 min each time in PBS–0.01% Tween 20 (PBS-T), incubated with a secondary Alexa 568-conjugated antibody (Molecular Probes; Invitrogen), washed, stained briefly in DAPI (4′,6′diamidino-2-phenylindole) solution (Sigma) (1:1,000 in PBS-T), washed again, and postfixed for 15 min in 4% (vol/vol) formaldehyde. Coverslips were mounted on microscope slides with Vectashield (Vector Laboratories, Burlingame, CA), and images were recorded on a Leica TCS-SPE confocal microscope and processed with Adobe Photoshop software.

Iodide efflux assay. A CFTR-mediated iodide efflux assay was adapted from previously described methods (24, 39, 51). BHK-21 cells were grown in 6-well dishes, transfected in duplicate experiments as indicated, and, 20 h later, washed twice and incubated for 30 min at 37°C in prewarmed iodide loading buffer (ILB) [136 mM NaI, 3 mM KNO_3, 2 mM $Ca(NO_3)_2$, 0.5 mM $MgSO_4$, 10 mM glucose, 20 mM HEPES (pH 7.5)]. Cells were then washed four times with efflux buffer (EB) [136 mM $NaNO_3$, 3 mM KNO_3, 2 mM $Ca(NO_3)_2$, 0.5 mM $MgSO_4$, 10 mM glucose, 20 mM HEPES (pH 7.5)] to completely remove extracellular iodide. Next, cells were left for equilibration during 10 min at 37°C in EB (first set of replicates) or in EB containing 10 μM cell-permeable CFTR-specific inhibitor 172 (Merck4Biosciences) (second set of replicates) before 10 μM forskolin and 50 μM IBMX (3-isobutyl-1-methylxanthine) (both from Sigma) were added for 5 min to allow protein kinase A-dependent CFTR stimulation. The presence of 10 μM CFTR inhibitor 172 (second set of replicate experiments) allowed correcting for endogenous non-CFTR-mediated iodide efflux activities and inhibited overall iodide efflux production by over 95%. Cells from all replicates were then quickly washed with fresh EB and the dishes completely drained. Cells were lysed for 5 min in 1 ml of EB–0.5% Triton X-100 (Sigma), scraped, and centrifuged at 16,000 × *g* for 5 min. Two sample aliquots were removed to quantify CFTR by Western blot analysis and total protein by the use of Precision Red protein assay reagent (Cytoskeleton, Denver, CO). The iodide content of the lysates was then determined using an iodide-selective electrode (Consort) connected to an MP225 general-purpose meter (Mettler Toledo) measuring the voltage differences. Sample voltages generated by the iodide in solution were interpolated from the standard curve generated by measuring 1, 10, 50, and 100 μM standard solutions and normalized to the amount of protein in the sample. The levels of iodide produced by efflux from transfected cells were calculated as the differences between the amounts of iodide remaining in inhibitor-172-treated versus nontreated replicate experiments; values are expressed in nanomoles. The statistical significance of the data was analyzed using two-tailed Student's *t* tests (Excel) as well as analysis of variance (ANOVA) with Tukey-Kramer's test (VassarStats [http://faculty.vassar.edu/lowry/VassarStats.html]).

RESULTS

WNK4 modulates the cell surface abundance of CFTR in mammalian cells. WNK4 can regulate various ion channels in a kinase-dependent or -independent manner, and one previous report identified a role in the expression of CFTR at the cell surface of *Xenopus* oocytes (48). In order to confirm this effect in mammalian cells, we used baby hamster kidney (BHK-21) cells engineered to stably express human CFTR protein (BHK-21-CFTR) (26, 38). Those cells have been used to create a well-characterized model system in the field and were transfected with GFP empty vector, the GFP-WNK4 wild type (WNK4-wt), or a GFP-WNK4 kinase-dead (WNK4-kd) mutant. The consequences for the CFTR protein were subsequently analyzed by three different techniques. First, cell surface proteins were labeled by biotinylation and isolated from cell lysates by the use of streptavidin beads. As shown in Fig. 1A, expression of both WNK4-wt and WNK4-kd increased the amount of CFTR detected at the cell surface, indicating that the underlying

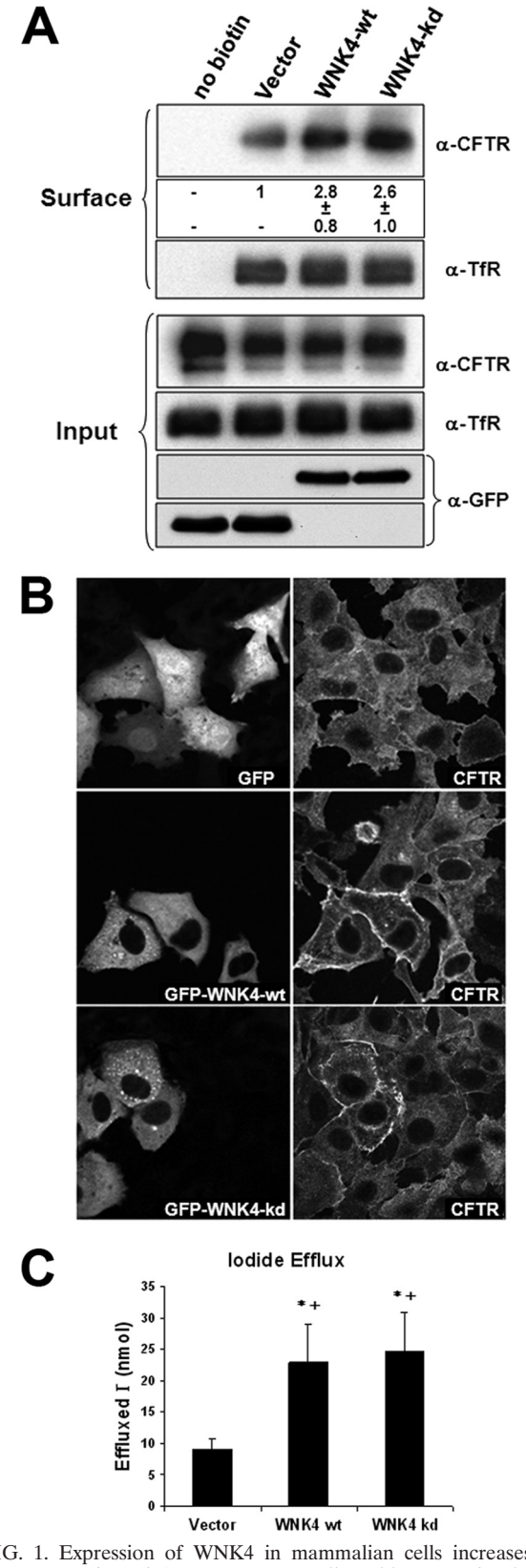

FIG. 1. Expression of WNK4 in mammalian cells increases cell surface expression of CFTR. BHK-21 cells stably expressing human CFTR protein were transfected with GFP-tagged expression vectors encoding GFP alone (vector) or WNK4 wild type (wt) or its kinase-dead mutant WNK4-kd and then analyzed by different techniques for changes in the cell surface expression of CFTR. (A) Biotinylation of cell surface proteins. Representative Western blots from a total of 7 independent experiments are shown, demonstrating the presence of CFTR protein and the transferrin receptor (TfR) either in the fraction of biotinylated cell surface proteins following pulldown with streptavidin beads (Surface) or in whole-cell lysates (Input). The differences in CFTR band intensities were quantified and are given below the blot as severalfold increases over control values ± standard deviations. No changes were observed in the case of the transferrin receptor. Cell lysates were further stained to document the expression levels of transfected GFP, GFP-WNK4-wt, or GFP-WNK4-kd. (B) Confocal immunofluorescence microscopy. In order to demonstrate qualitatively the effect on CFTR surface expression, the indicated GFP-tagged vectors were diluted so that most microscopic fields contained transfected and nontransfected cells side by side. Cells were fixed and stained with anti-CFTR antibody 570 followed by anti-mouse Alexa 568 conjugate. Images were recorded sequentially for DAPI, GFP, and Alexa stainings. GFP-positive cells represent the successfully transfected cells. (C) CFTR-mediated ion transport by iodide efflux (for details, see Materials and Methods). The statistical significance of the differences was determined using both two-tailed Student's *t* tests (*, $P < 0.0001$) and ANOVA ($P < 0.0001$, comparing the three sample groups) followed by Tukey-Kramer's test (+, $P < 0.01$ compared to the control). All experiments were repeated in at least three independent transfection assays.

effect is not dependent on catalytic kinase activity. Under the same experimental conditions, the cell surface levels of endogenous transferrin receptor 1 (TfR1) did not change (Fig. 1A). We confirmed that the biotinylation reaction did not label cytosolic proteins such as tubulin (data not shown) and that transfection of GFP empty vector did not alter the steady-state CFTR surface levels.

Second, confocal immunofluorescence microscopy analysis confirmed an increase in CFTR staining at the cell surface in WNK4-wt- or WNK4-kd-transfected cells (Fig. 1B). Third, CFTR-mediated ion transport activity in transfected cells was determined by an iodide efflux assay following correction for endogenous non-CFTR-mediated iodide efflux activities through normalization against a parallel set of cells treated with CFTR inhibitor 172. These activity assays revealed a roughly 2-fold increase in iodide release upon WNK4-wt or WNK4-kd expression (Fig. 1C).

WNK4 exists in a complex with spleen tyrosine kinase (Syk). In order to identify the molecular mechanism underlying this effect of WNK4 on CFTR surface expression, we screened proteins interacting with WNK4 by the use of an antibody array. To this end, HEK293 cells were transfected with Myc-tagged WNK4 and lysed under nondenaturing conditions to preserve protein-protein interactions, and the extract was incubated with the antibody array. Briefly, the array contained antibodies against 400 cellular proteins involved in signal transduction that are able to bind their cognate proteins from the cell lysate. Those proteins forming a complex with Myc-WNK4 in the lysate were revealed by chemiluminescence staining of the array membrane with an anti-Myc peroxidase conjugate. After subtraction of unspecific signals generated by the anti-Myc antibody alone, one clear positive hit for WNK4 was obtained at the position of anti-spleen tyrosine kinase (Syk) (Fig. 2A).

For confirmation of the observed interaction, Myc-WNK4 and YFP-Syk were cotransfected into HEK293 cells (as well

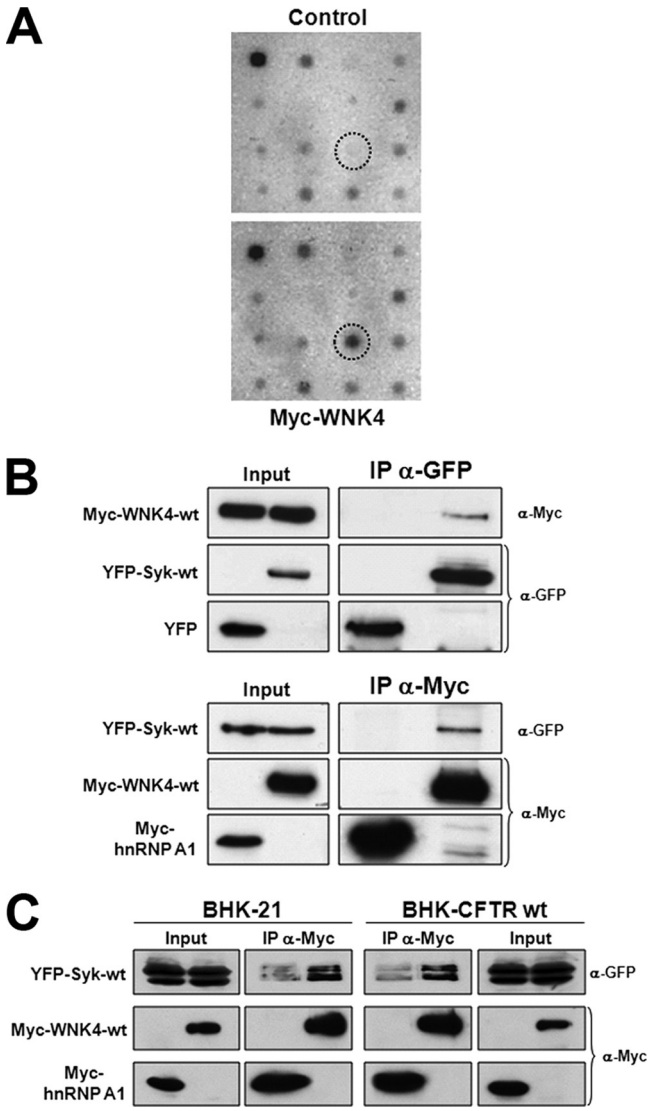

FIG. 2. WNK4 forms a protein complex with Syk protein kinase. (A) Identification of Syk as a WNK4-interacting protein by the use of an antibody array. Lysates of HEK293 cells transfected with either Myc-WNK4-wt or empty vector (Control) were incubated with an antibody array. WNK4-protein interactions were then revealed by chemiluminescence using an anti-Myc peroxidase-conjugated antibody. The relevant array areas are shown with one WNK4-specific signal that corresponded to the position of Syk (circle). (B) Coimmunoprecipitation experiments to confirm the observed WNK4-Syk interaction. HEK293 cells were cotransfected with Myc-WNK4-wt and YFP-Syk-wt as well as with YFP alone and Myc-hnRNP A1 as controls, lysed under nondenaturing conditions, and incubated with either anti-GFP antibodies to precipitate Syk (top panels) or with anti-Myc antibodies to precipitate WNK4 (bottom panels). Results of Western blot analyses of the expression levels in whole-cell lysates (Input) and the immunoprecipitated fractions (IP) are shown. As respective controls, the YFP protein and Myc-tagged-hnRNP A1 were used. Note that immunoprecipitated YFP-Syk pulls down WNK4 and, in contrast, that immunoprecipitates of Myc-WNK4 revealed the presence of Syk. (C) Validation of the observed interaction in CFTR-expressing BHK-21 cells. Parental and CFTR-expressing BHK-21 cells were cotransfected with YFP-Syk-wt and either Myc-WNK4-wt or Myc-hnRNP A1 (control). Myc-tagged proteins were immunoprecipitated and analyzed by Western blotting as described above. All experiments were repeated in at least three independent transfection assays.

as GFP alone and Myc-hnRNP A1 as respective controls) and immunoprecipitated. Anti-GFP antibodies immunoprecipitated Syk, and the presence of WNK4 was clearly detected in the YFP-Syk precipitate but not with YFP alone. In contrast, anti-Myc antibodies precipitated WNK4 and the presence of Syk was detected with anti-YFP antibodies. Also, as a control, the unrelated nuclear protein Myc-hnRNP A1 was expressed but did not coimmunoprecipitate with Syk (Fig. 2B). The endogenous WNK4 protein could not be immunoprecipitated due to a lack of suitable commercial antibodies.

Because HEK293 cells do not express endogenous CFTR protein, the coimmunoprecipitation studies were repeated with parental and CFTR-expressing BHK-21 cells. The results confirmed that Syk precipitated specifically with Myc-WNK4 but not with Myc-hnRNP A1 and that this interaction occurred independently of the presence of the CFTR protein (Fig. 2C).

Syk forms a complex with CFTR and phosphorylates the NBD1 domain *in vitro*. Because no functional interaction between protein kinase Syk and CFTR has been described to date, we first tested whether the two proteins were able to coimmunoprecipitate. BHK-21-CFTR cells were transfected to express either YFP protein or YFP-Syk, and both were immunoprecipitated from cell lysates by the use of the anti-GFP antibody. The precipitates revealed the presence of CFTR protein only in the case of YFP-Syk (Fig. 3A).

We then tested whether the CFTR protein was a Syk substrate *in vitro*. BHK-21-CFTR cells were lysed under stringent SDS-containing RIPA buffer conditions to immunoprecipitate the CFTR protein, which was then preincubated with unlabeled ATP to saturate potential contaminating phosphorylation activities. Independently, YFP-Syk-wt or a kinase-dead mutant (YFP-Syk-kd) was immunoprecipitated from transfected cells in RIPA buffer so that contamination with other kinases from the cell lysate was minimized. The beads were then washed in protein kinase buffer, added to the CFTR beads, and incubated in the presence of radioactive ATP and inhibitors of protein serine/threonine kinases known to phosphorylate CFTR (1). As shown in Fig. 3B, Syk-wt autophosphorylated and phosphorylated CFTR whereas Syk-kd showed no such activities.

We analyzed the CFTR peptide sequence and found a single Syk recognition motif (Y-D/E-D/E-X) at Tyr512 in the first nucleotide binding domain (NBD1) (Fig. 3C). We thus tested next whether Syk could phosphorylate the NBD domain at Tyr512 *in vitro*. YFP-Syk-wt or YFP-Syk-kd was immunoprecipitated as described above, and the beads were washed in protein kinase buffer and incubated with radioactive ATP in the presence of isolated NBD1 as a substrate. In a first set of experiments, recombinant NBD1 (kind gift of P. J. Thomas) was found to be phosphorylated by Syk-wt but not by Syk-kd (Fig. 4, left panels). In order to demonstrate that Tyr512 was indeed the residue targeted by this activity, the NBD1 coding sequence was point mutated to a phenylalanine at position 512 and then expressed as Sumo-tagged recombinant protein in order to yield acceptable amounts of soluble mutant NBD1. While Syk clearly phosphorylated Sumo-NBD1-wt, it no longer phosphorylated the NBD1-Y512F mutant (Fig. 4, middle panels). Since the phosphorylation of recombinant proteins *in vitro* can sometimes result from an incorrect conformation, we confirmed these data using the Myc-tagged NBD1 domain expressed in HEK293 cells as a substrate for the Syk kinase

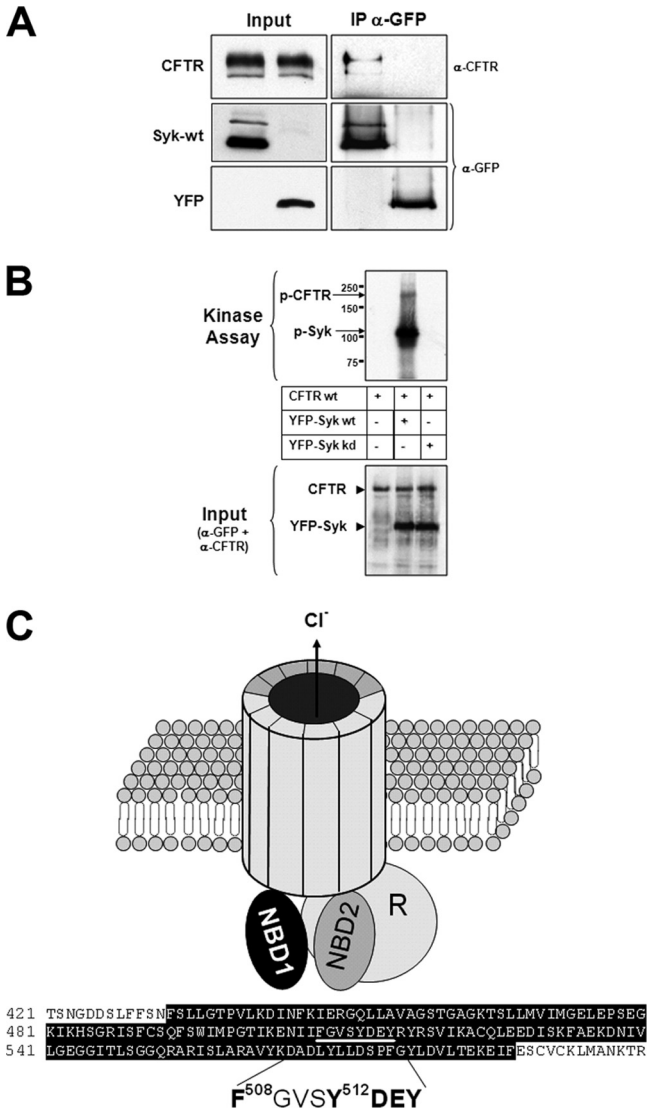

FIG. 3. CFTR is a substrate for Syk protein kinase and contains a Syk substrate motif in the NBD1 domain. (A) CFTR coimmunoprecipitates with Syk. YFP vector or YFP-Syk-wt was transfected into CFTR-expressing BHK-21 cells and immunoprecipitated with anti-GFP antibodies. Whole-cell lysates and precipitates were then separated in acrylamide gels optimized for the best resolution of CFTR bands B and C. Western blots revealing the expression levels of YFP, YFP-Syk (anti-GFP), and CFTR (rabbit anti-CFTR Lis1) in whole-cell lysates (Input) and in the immunoprecipitated fractions (IP) are shown. Note that only YFP-Syk coprecipitated the CFTR protein. The second visible Syk protein band occurred as an effect of the CFTR-specific gel conditions. (B) CFTR is a substrate for protein kinase Syk. Full-length CFTR protein was immunoprecipitated with antibody clone 570 from BHK-21-CFTR cells and then mixed with radioactive ATP and beads containing either Syk-wt or Syk-kd mutant. To reduce nonspecific background phosphorylation, the immunoprecipitated CFTR protein was premixed with unlabeled ATP and then assayed in the presence of protein serine/threonine kinase inhibitors. Samples were separated by gel electrophoresis and transferred to PVDF blotting membranes, and the membranes were exposed to X-ray films (Kinase Assay) detecting incorporated radioactive [^{32}P]phosphate, followed by Western blot analysis to document the levels of immunoprecipitated proteins (Input). Note that only Syk-wt was able to phosphorylate CFTR as well as to autophosphorylate. (C) Model of the CFTR ion channel structure with 12 transmembrane domains, two nucleotide-binding domains (NBD), and a regulatory domain (R). Below the model, the sequence of the cytoplasmic nucleotide binding-domain 1 (NBD1) is highlighted in black; the relevant residues containing the Syk substrate motif are underlined and shown in greater detail below the sequence. Note that tyrosine 512 is close to phenylalanine 508, the residue most frequently mutated in cystic fibrosis patients.

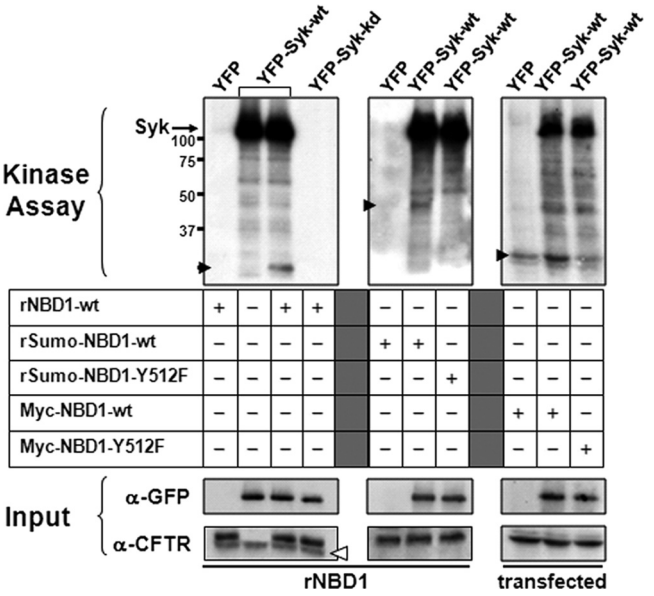

FIG. 4. Syk phosphorylates the CFTR NBD1 domain *in vitro*. YFP vector or YFP-Syk-wt or YFP-Syk-kd was transfected into HEK293 cells, immunoprecipitated, and tested in *in vitro* protein kinase assays for the ability to phosphorylate CFTR. The added substrates were recombinant NBD1 domain (left panels), Sumo-tagged recombinant NBD1 or its Y512F derivative (middle panels), or transfected Myc-tagged NBD1 or Myc-NBD1-Y512F (right panels) immunoprecipitated from HEK293 cells. Samples were separated by gel electrophoresis and transferred to PVDF blotting membranes. Images from X-ray films (Kinase Assay) detecting radiolabeled proteins are shown; black arrowheads indicate the positions of NBD1 detected with anti-CFTR clone L12B4 on a subsequent Western blot. Note that Syk-wt (but not the Syk-kd mutant) phosphorylates NBD1 (besides Syk autophosphorylation) and that phosphorylation by Syk is abolished after mutating Y512 to phenylalanine (F). Phosphorylation of Myc-tagged NBD1 was 2.6-fold higher in the presence of Syk-wt than in the presence of vector alone or NBD1-Y512F background levels. In order to document equal quantities of immunoprecipitated Syk or NBD1 substrate protein, membranes were subsequently subjected to immunostaining with anti-GFP and anti-CFTR antibody L12B40 (Input). The white arrowhead indicates the position of immunoglobulin light chains which retained some radioactive phosphate. Experiments were repeated in at least three independent assays.

assay. Whereas the immunoprecipitated Myc-NBD1 domain was found to be phosphorylated by Syk *in vitro*, the corresponding NBD1-Y512F mutant was not recognized as a substrate (Fig. 4, right panels). Although this approach does not guarantee that Syk recognizes the isolated NBD1 with the same efficiency as full-length CFTR, the results confirmed qualitatively that Syk can phosphorylate only the wt but not NBD1-Y512F.

WNK4 inhibits NBD1 phosphorylation by Syk. Since, as described above, we found that Syk interacts with WNK4, we tested the effect of WNK4 on NBD1 phosphorylation by Syk.

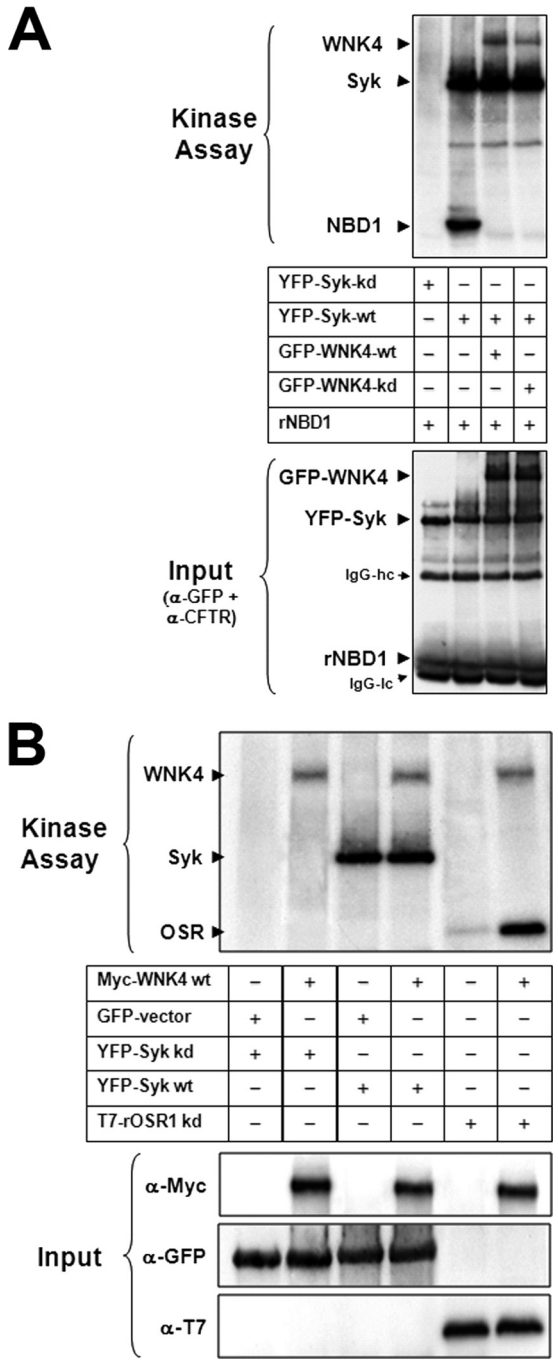

FIG. 5. WNK4 inhibits Syk-mediated NBD1 phosphorylation. (A) WNK4 inhibits NBD1 phosphorylation by Syk. YFP-Syk-wt, YFP-Syk-kd, GFP-WNK4-wt, or GFP-WNK4-kd was transfected into HEK293 cells, immunoprecipitated, and pooled as indicated to test for the ability to phosphorylate recombinant NBD1 in *in vitro* protein kinase assays. Samples were separated and analyzed as described in the legend to Fig. 3B. Note that Syk and WNK4 autophosphorylate and that the presence of WNK4 prevents Syk from phosphorylating NBD1. (B) WNK4 does not phosphorylate Syk *in vitro*. YFP-Syk-wt, YFP-Syk-kd, or Myc-WNK4-wt was transfected into HEK293 cells, immunoprecipitated, and pooled as indicated for *in vitro* protein kinase assays. As a positive control, Myc-WNK4-wt was incubated with recombinant OSR1, a previously described substrate. Samples were separated and analyzed as described in the legend to Fig. 4. Note that WNK4 phosphorylates OSR1 but not the Syk proteins. Experiments were repeated in at least three independent assays.

For this purpose, Myc-WNK4-wt or WNK4-kd was expressed, immunoprecipitated, and added to Syk-wt and recombinant NBD1 in the *in vitro* kinase assay. It was found that the presence of either WNK4-wt or WNK4-kd completely prevented Syk from phosphorylating NBD1 (Fig. 5A). In order to further study how WNK4 inhibits the NBD1 phosphorylation by Syk, we analyzed whether WNK4 could directly phosphorylate Syk *in vitro*. Myc-WNK4-wt was expressed in cells, immunoprecipitated, and mixed in *in vitro* kinase assays with either Syk-wt or Syk-kd. As a positive control, recombinant OSR1 was added as a known WNK substrate (44) and found to become phosphorylated by WNK4 (Fig. 5B). In contrast, Syk-kd was not phosphorylated by WNK4, and Syk-wt revealed only its own autophosphorylation level without any evidence for additional phosphorylation by WNK4.

Syk activity modulates the expression of CFTR at the cell surface. Since Syk phosphorylated the NBD1 domain of CFTR *in vitro*, we asked whether Syk can modulate the expression of CFTR at the cell surface. Thus, BHK-21-CFTR cells were transfected with YFP-tagged expression vectors encoding YFP alone (vector), Syk-wt, or Syk-kd and then analyzed for expression of CFTR at the cell surface by biotinylation of cell surface proteins, immunofluorescence microscopy, and iodide efflux assays, all in comparison to the described effect of wt WNK4. Expression of Syk-wt led to a decrease in the amount of CFTR at the cell surface both as biotinylated protein (Fig. 6A) and as revealed by immunofluorescence staining (Fig. 6B). In contrast, expression of Syk-kd increased the amounts of plasma membrane-associated CFTR in both assays to levels comparable to those obtained upon expression of WNK4-wt. These data were confirmed by iodide efflux measurements (Fig. 6C) demonstrating that the observed changes in surface amounts of CFTR reflected different capacities of the cells to produce iodide efflux upon forskolin-IBMX stimulation.

Endogenous Syk and WNK4 regulate CFTR surface expression in human airway epithelial cells. In order to test the physiologic relevance of our findings, we validated the effect of Syk and WNK4 in the CF-bronchial epithelial cell line CFBE41o- (wt-CFBE) (3). These cells were found to express endogenous Syk and WNK4, and their respective expression levels were successfully reduced upon transfection with specific siRNAs within 48 h (Fig. 7A). Transfected wt-CFBE cells were thus analyzed by biotinylation of cell surface proteins to determine the expression levels of CFTR at the cell surface under these conditions. As shown in Fig. 7B, the downregulation of Syk promoted CFTR surface levels, thus confirming the inhibitory role in this process that we identified above. In contrast, the depletion of endogenous WNK4, which we found to antagonize Syk as described above, led to a clear decrease in CFTR levels at the cell surface. Under the same experimental conditions, the cell surface levels of the endogenous transferrin receptor (TfR) did not change (Fig. 7B).

Mutation of tyrosine 512 is sufficient to promote changes in the expression of CFTR at the cell surface. In order to demonstrate that the observed phosphorylation in the NBD1 domain is functionally relevant *in vivo*, Tyr512 was changed by site-directed mutagenesis into either nonphosphorylatable Phe or a phosphomimetic Glu residue. These CFTR mutants were stably transfected into parental BHK-21 cells, and CFTR activity was measured by the iodide efflux technique (Fig. 8A).

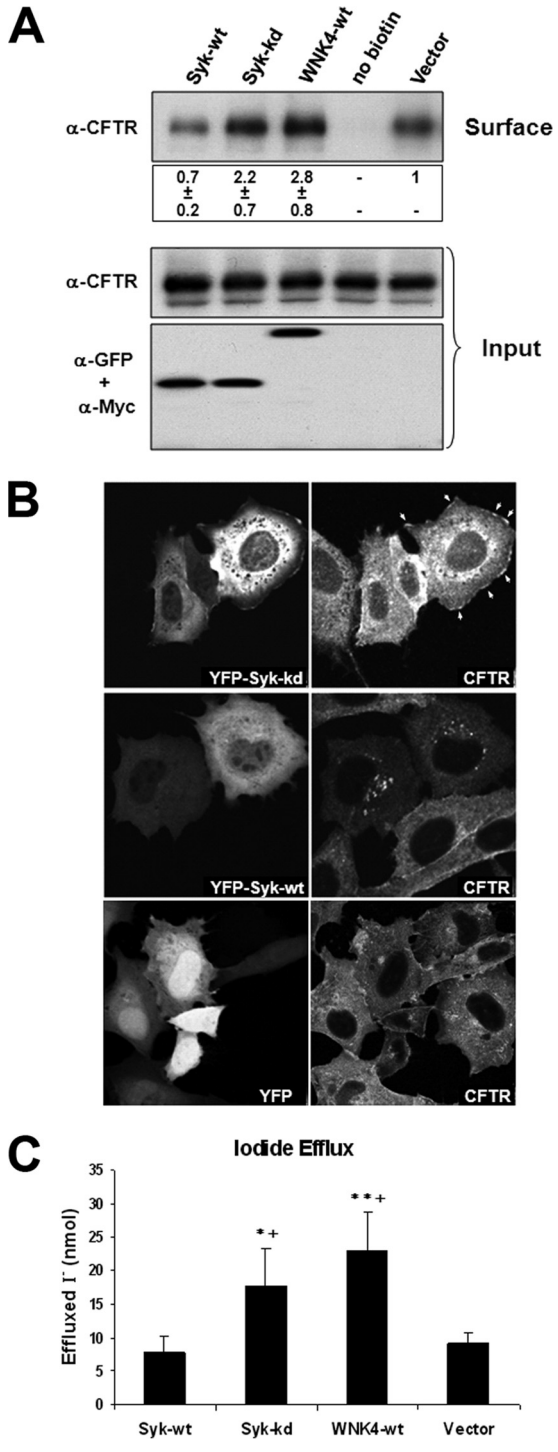

FIG. 6. WNK4 and Syk have antagonistic effects on the cell surface expression of CFTR. BHK-21-CFTR cells were transiently transfected with GFP-tagged expression vectors encoding YFP alone (vector), WNK4-wt, Syk-wt, or Syk-kd and then analyzed by different techniques for changes in expression levels of CFTR at the cell surface (for more details, see the legend to Fig. 1). (A) Biotinylation of cell surface proteins. (B) Confocal immunofluorescence microscopy. YFP-positive cells represent the successfully transfected cells. (C) CFTR-mediated ion transport by iodide efflux. Note that expression of Syk-wt decreased whereas that of Syk-kd or WNK4-wt increased surface CFTR levels compared to control cell results. Experiments were repeated in at least three independent transfection assays. The statistical significance of the differences was determined using both two-tailed Student's *t* tests (*, $P < 0.006$; **, $P < 0.0001$) and ANOVA ($P < 0.0001$, comparing the four sample groups) followed by Tukey-Kramer's test (+, $P < 0.01$ compared to control results).

CFTR-Y512E-expressing cells showed a significant decrease in CFTR-mediated ion transport, whereas cells expressing CFTR Y512F released almost twice the amount of iodide as wt CFTR-expressing cells. These data were found to correlate to the increased amount of biotinylated CFTR protein at the cell surface compared to that seen with BHK-21-CFTR cells (Fig. 8B). These mutants thus mimic the effects on CFTR of transfecting either Syk-wt or Syk-kd. To further confirm that Tyr512 mediates the observed effects of Syk and WNK4 *in vivo*, we first cotransfected the cells with nonphosphorylatable CFTR-Y512F and YFP-Syk-wt. Surface biotinylation revealed that Syk-wt could no longer reduce CFTR-Y512F surface expression levels (Fig. 8B, middle two lanes). Second, cells were cotransfected with the phosphomimetic CFTR-Y512E mutant and Myc-WNK4-wt. Under these conditions, expression of WNK4 was unable to raise surface levels of the CFTR-Y512E mutant protein (Fig. 8B, right two lanes) to those seen with wt CFTR (second lane from left).

DISCUSSION

The data presented in this work provide two novel insights into the regulation of cell surface expression of CFTR. First, we show that the CFTR protein is a substrate for phosphorylation by protein kinase Syk at NBD1 residue Tyr512, leading to a reduction in the cell surface expression of CFTR. Second, we describe an antagonistic role for WNK4 and Syk in regulating the cell surface expression of CFTR.

In our experiments, Syk was initially identified as a WNK4 partner protein in HEK293 cells when proteins involved in signal transduction were screened for formation of complexes with Myc-WNK4 under nondenaturing conditions. The interaction was clearly confirmed by coimmunoprecipitation when either WNK4 or Syk was pulled down (Fig. 2). The observed interaction occurred in both human HEK293 and rodent BHK-21 cells and was independent of the presence of CFTR.

Because expression of WNK4 enhanced the amount of CFTR at the plasma membrane (Fig. 1), we searched for a possible role of Syk in this process and found a Syk phosphorylation motif at Tyr512 of the CFTR sequence, i.e., in its first nucleotide binding domain (NBD1). In protein kinase assays performed *in vitro*, this CFTR domain was indeed found to be phosphorylated by Syk at Tyr512. Furthermore, when Syk is overexpressed in cells, it associates with and coimmunoprecipitates CFTR, an interaction resulting in a slight reduction in the amount of cell surface biotinylated CFTR. Even more significant was the outcome of expression of a kinase-dead (dominant-negative) Syk mutant, which may interact with CFTR but not phosphorylate it; expression of the mutant caused a significant increase in the level of cell surface CFTR. This indicates that Syk activity normally restricts expression of CFTR at the plasma membrane. This increase in surface CFTR was confirmed by fluorescence microscopy and by measuring CFTR-

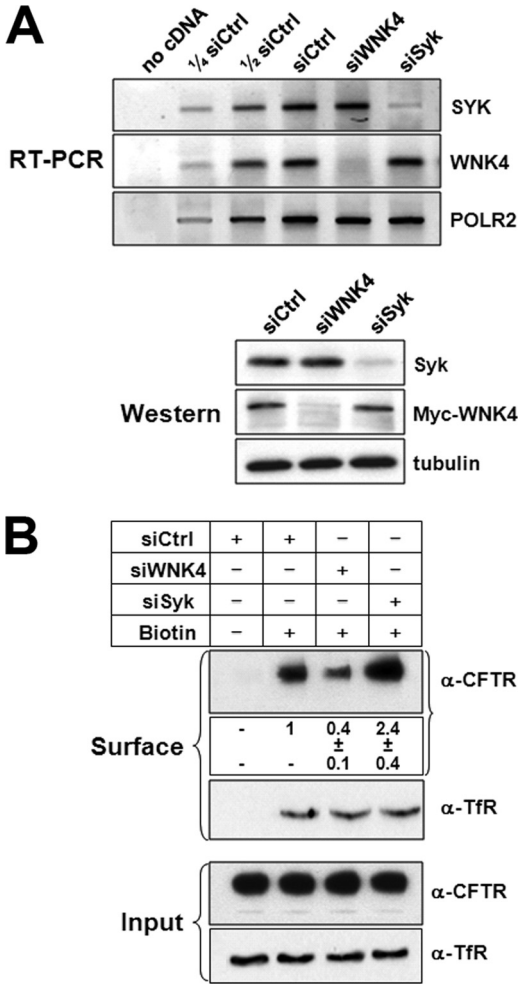

FIG. 7. Endogenous WNK4 and Syk affect the cell surface expression of CFTR in bronchial epithelial cells. Human wt-CFBE cells were transiently transfected with small interfering RNA (siRNA) oligonucleotides to downregulate the endogenous expression of either Syk or WNK4. (A) Expression levels of Syk and WNK4 determined by RT-PCR and agarose gel electrophoresis as well as downregulation of the corresponding transcripts after 48 h are shown. Two serial 2-fold dilutions of the control sample were also loaded to allow estimation of the degree of depletion (top panels). Western blot confirmation of protein downregulation was possible only for endogenous Syk due to the lack of suitable anti-human WNK4 antibodies. However, the efficiency of si-RNA-mediated depletion of WNK4 protein was clearly demonstrated using transfected Myc-WNK4 (bottom panels). (B) Biotinylation of cell surface proteins. The effect of Syk or WNK4 depletion on changes in cell surface expression of CFTR and TfR was determined by Western blot analysis, as described in the legend to Fig. 1. Note that surface CFTR levels increased upon downregulation of Syk expression, whereas in the case of WNK4, the amount of channel at the cell surface decreased compared to control cell results. Under these conditions, TfR surface levels were not affected.

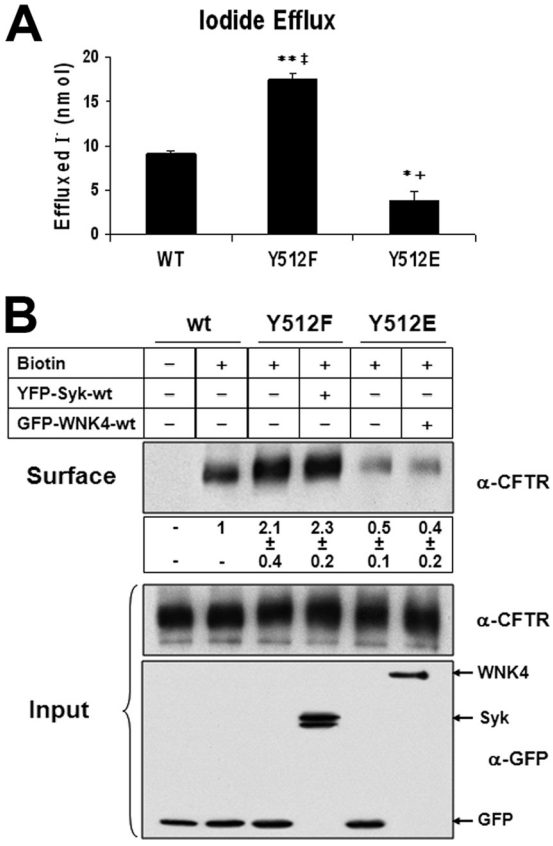

FIG. 8. The presence of phosphomimetic mutants of CFTR tyrosine 512 is sufficient to change CFTR cell surface expression. BHK-21 cells were stably transfected with CFTR mutant constructs carrying point mutations in tyrosine 512 so that either a phosphomimetic glutamic acid residue (Y512E) or an unphosphorylatable phenylalanine residue (Y512F) was present. Cells were analyzed by different techniques for determination of changes in levels of expression of CFTR at the cell surface, as described in the legend to Fig. 1. (A) CFTR-mediated ion transport by iodide efflux. The statistical significance of the differences was determined using both two-tailed Student's *t* tests (*, $P < 0.03$; **, $P < 0.005$) and ANOVA ($P < 0.0001$, comparing the three sample groups) followed by Tukey-Kramer's test (+, $P < 0.05$; ‡, $P < 0.01$ [for comparisons to wt results]). (B) Biotinylation of cell surface proteins. Note that CFTR-Y512E is less abundant but that CFTR-Y512F is more abundant at the cell surface than wt CFTR. In addition, it was no longer possible to decrease the surface abundance of CFTR-Y512F by transfection of YFP-Syk-wt, and the abundance of CFTR-Y512E was no longer increased by expression of GFP-WNK4-wt.

mediated iodide efflux levels in living cells (Fig. 6). Finally, CFTR mutations mimicking either a constitutive phosphorylated or a nonphosphorylated Tyr512 were sufficient to provoke the corresponding changes in the CFTR cell surface abundance and iodide efflux levels (Fig. 8).

Together, these data make a convincing case that phosphorylation of CFTR at Tyr512 by Syk is a novel regulatory mechanism to modulate the amount of CFTR present at the plasma membrane. Although serine/threonine phosphorylation of CFTR was known to occur in the regulatory domain of CFTR, leading to channel opening and activation of transport activity (11), our data on Syk reveal a previously unknown role for tyrosine phosphorylation in the NBD1 domain and a role in the regulation of CFTR expression at the cell surface. Our data further reveal that WNK4 acts in a manner antagonistic to Syk and promotes surface expression of CFTR.

The physiological relevance of these findings is strongly supported by the fact that endogenous expression of Syk and WNK4 was detected in airway epithelial cells and that their experimental downregulation clearly affected CFTR cell sur-

face expression (Fig. 7). These experiments confirmed that Syk has an inhibitory role with respect to CFTR surface levels and that WNK4 positively regulates these. Expression of Syk in primary or transformed human bronchial epithelial cells was also previously confirmed by others (42). A previous analysis of WNK4 in extrarenal tissues found expression in lung and other chloride-transporting epithelia, including sweat ducts, colonic crypts, pancreatic ducts, and epididymis (19). Thus, the tissue-specific WNK4 expression pattern largely overlaps with that of CFTR. Given that WNK kinases can be activated by changes in extracellular osmolarity (21), it is tempting to postulate that WNK4 responds to fluctuations of the airway surface fluid and adjusts the amount of CFTR activity accordingly.

The *in vitro* phosphorylation of CFTR NBD1 at Tyr512 by Syk was inhibited by WNK4-wt as well as by its WNK4-kd mutant. Thus, the inhibition was most likely mediated by the protein-protein interaction that we observed between Syk and WNK4, the molecular details of which remain to be determined. Other WNK4-mediated effects on ion channels were also previously described as independent of the presence of kinase and include the inhibition of ROMK (22) and of ENaC (34) surface expression in *Xenopus* oocytes. In both cases, changes in the endocytosis of the respective channels are involved, albeit through different molecular pathways: while the inhibitory effect of WNK4 on ROMK involves binding to the linker protein intersectin to facilitate clathrin-dependent endocytosis (15), the downregulation of ENaC is most likely mediated by the E3 ubiquitin ligase Nedd4-2 to direct ENaC into the lysosomal pathway for degradation (34). Whether the antagonistic effects of WNK4 and Syk on CFTR also involve endocytosis or instead involve changes in membrane traffic and CFTR delivery remains to be determined; however, the effect of WNK4 on CFTR surface levels is clearly specific, because no changes in endogenous transferrin receptor surface levels were observed under the same experimental conditions (Fig. 1A and 7B). Intriguingly, when we expressed the Syk-kd mutant, leading to an increase in surface CFTR levels, our immunofluorescence analysis revealed that this mutant colocalized at the plasma membrane with sites of increased CFTR staining (Fig. 6B). This suggests that, under normal conditions, Syk is recruited to the plasma membrane by CFTR and then phosphorylates it, triggering CFTR endocytosis. The presence of WNK4 would then sequester Syk and increase retention of CFTR at the cell surface. The upstream signals regulating activation or expression of Syk and WNK4 remain to be determined.

Our findings have several remarkable implications. First, the WNK4/Syk interplay identified for CFTR may also operate in the regulation of other chloride cotransporters. Given that an increase in apical CFTR activity would require concomitant activation of basolateral ion channels to coordinate transepithelial chloride flux (20), it is tempting to speculate that WNK4 and/or Syk controls this coordination. Second, the WNK4/Syk pathway may be of therapeutic interest for patients with cystic fibrosis. The most frequent mutation in patients is deletion of phenylalanine 508, which causes increased proteolytic degradation of the misfolded mutant CFTR protein. Interestingly, however, the mutant protein exhibits some residual chloride channel activity and could partially reduce disease severity if its retention at the plasma membrane were improved (2). Because our data suggest that Syk normally inhibits CFTR surface expression, a relevant topic in future studies might be the inhibition of Syk to favor the prevalence at the plasma membrane of mutant CFTR proteins retaining some chloride channel activity (e.g., F508del-CFTR). Third, Syk inhibitors may be beneficial in cystic fibrosis therapy, because the disease is characterized by chronic lung inflammation due to impaired clearance of the thick mucus that forms in the absence of CFTR-mediated chloride transport (4). Syk inhibitors are currently used in the clinic to inhibit inflammation and treat allergic rhinitis and rheumatoid arthritis (36, 40). The efficacy of such treatment in due to the role of Syk in immunoreceptor signaling in leukocytes (27, 36), but recent studies have suggested that Syk also functions in tumor necrosis factor-induced nitric oxide production by airway epithelial cells (41).

ACKNOWLEDGMENTS

For kindly providing reagents used in this study, we thank H. König, (Karlsruhe, Germany) for Myc-hnRNP A1, X. Jeunemaître (Paris, France) for human WNK4 and WNK4-K174A cDNAs, Philip J. Thomas (University of Texas Southwestern Medical Center, Dallas, TX) and the CFTR Folding Consortium (CFF; Bethesda, MD) for recombinant NBD1 and vector pET-Sumo-NBD1, and J. P. Clancy (University of Alabama, Birmingham) for the wt-CFBE cell line.

This work was supported by the Portuguese Fundação para a Ciência e Tecnologia (grants POCI_PPCDT/SAU-MMO/56439/04 and PTDC/BIA-BCM/67058/06, Programa de Financiamento Pluri-anual do BioFIG (PEst-OE/BIA/UI4046/2011), and fellowships BD/23001/05 to A.I.M. and BPD/47445/08 to S.M.).

REFERENCES

1. **Alzamora, R., J. D. King, Jr., and K. R. Hallows.** 2011. CFTR Regulation by phosphorylation. Methods Mol. Biol. **741:**471–488.
2. **Amaral, M. D.** 2005. Processing of CFTR: traversing the cellular maze—how much CFTR needs to go through to avoid cystic fibrosis? Pediatr. Pulmonol. **39:**479–491.
3. **Bebok, Z., et al.** 2005. Failure of cAMP agonists to activate rescued deltaF508 CFTR in CFBE41o- airway epithelial monolayers. J. Physiol. **569:**601–615.
4. **Belcher, C. N., and N. Vij.** 2010. Protein processing and inflammatory signaling in cystic fibrosis: challenges and therapeutic strategies. Curr. Mol. Med. **10:**82–94.
5. **Cai, H., et al.** 2006. WNK4 kinase regulates surface expression of the human sodium chloride cotransporter in mammalian cells. Kidney Int. **69:**2162–2170.
6. **Camerino, D. C., J. F. Desaphy, D. Tricarico, S. Pierno, and A. Liantonio.** 2008. Therapeutic approaches to ion channel diseases. Adv. Genet. **64:**81–145.
7. **Cha, S. K., and C. L. Huang.** 2010. WNK4 kinase stimulates caveola-mediated endocytosis of TRPV5 amplifying the dynamic range of regulation of the channel by protein kinase C. J. Biol. Chem. **285:**6604–6611.
8. **Dorwart, M. R., N. Shcheynikov, Y. Wang, S. Stippec, and S. Muallem.** 2007. SLC26A9 is a Cl(-) channel regulated by the WNK kinases. J. Physiol. **584:**333–345.
9. **Farinha, C. M., F. Mendes, M. Roxo-Rosa, D. Penque, and M. D. Amaral.** 2004. A comparison of 14 antibodies for the biochemical detection of the cystic fibrosis transmembrane conductance regulator protein. Mol. Cell. Probes **18:**235–242.
10. **Fu, Y., A. Subramanya, D. Rozansky, and D. M. Cohen.** 2006. WNK kinases influence TRPV4 channel function and localization. Am. J. Physiol. Renal Physiol. **290:**F1305–F1314.
11. **Gadsby, D. C., and A. C. Nairn.** 1999. Control of CFTR channel gating by phosphorylation and nucleotide hydrolysis. Physiol. Rev. **79**(Suppl. 1)**:**S77–S107.
12. **Gagnon, K. B., R. England, and E. Delpire.** 2006. Volume sensitivity of cation-Cl- cotransporters is modulated by the interaction of two kinases: Ste20-related proline-alanine-rich kinase and WNK4. Am. J. Physiol. Cell Physiol. **290:**C134–C142.
13. **Gamba, G.** 2005. Role of WNK kinases in regulating tubular salt and potassium transport and in the development of hypertension. Am. J. Physiol. Renal Physiol. **288:**F245–F252.
14. **Golbang, A. P., et al.** 2006. Regulation of the expression of the Na/Cl cotransporter by WNK4 and WNK1: evidence that accelerated dynamin-

dependent endocytosis is not involved. Am. J. Physiol. Renal Physiol. **291:** F1369–F1376.
15. **He, G., H. R. Wang, S. K. Huang, and C. L. Huang.** 2007. Intersectin links WNK kinases to endocytosis of ROMK1. J. Clin. Invest. **117:**1078–1087.
16. **Heise, C. J., et al.** 2010. Serum and glucocorticoid-induced kinase (SGK) 1 and the epithelial sodium channel are regulated by multiple with no lysine (WNK) family members. J. Biol. Chem. **285:**25161–25167.
17. **Jentsch, T. J., C. A. Hübner, and J. C. Fuhrmann.** 2004. Ion channels: function unravelled by dysfunction. Nat. Cell Biol. **6:**1039–1047.
18. **Jiang, Y., W. B. Ferguson, and J. B. Peng.** 2007. WNK4 enhances TRPV5-mediated calcium transport: potential role in hypercalciuria of familial hyperkalemic hypertension caused by gene mutation of WNK4. Am. J. Physiol. Renal Physiol. **292:**F545–F554.
19. **Kahle, K. T., et al.** 2004. WNK4 regulates apical and basolateral Cl- flux in extrarenal epithelia. Proc. Natl. Acad. Sci. U. S. A. **101:**2064–2069.
20. **Kahle, K. T., et al.** 2006. WNK protein kinases modulate cellular Cl- flux by altering the phosphorylation state of the Na-K-Cl and K-Cl cotransporters. Physiology **21:**326–335.
21. **Kahle, K. T., A. M. Ring, and R. P. Lifton.** 2008. Molecular physiology of the WNK kinases. Annu. Rev. Physiol. **70:**329–355.
22. **Kahle, K. T., et al.** 2003. WNK4 regulates the balance between renal NaCl reabsorption and K+ secretion. Nat. Genet. **35:**372–376.
23. **Lalioti, M. D., et al.** 2006. Wnk4 controls blood pressure and potassium homeostasis via regulation of mass and activity of the distal convoluted tubule. Nat. Genet. **38:**1124–1132.
24. **Long, K. J., and K. B. Walsh.** 1997. Iodide efflux measurements with an iodide-selective electrode: a non-radioactive procedure for monitoring cellular chloride transport. Methods Cell Sci. **19:**207–212.
25. **Matter, N., et al.** 2000. Heterogeneous ribonucleoprotein A1 is part of an exon-specific splice-silencing complex controlled by oncogenic signaling pathways. J. Biol. Chem. **275:**35353–35360.
26. **Mendes, F., et al.** 2003. Unusually common cystic fibrosis mutation in Portugal encodes a misprocessed protein. Biochem. Biophys. Res. Commun. **311:**665–671.
27. **Mócsai, A., J. Ruland, and V. L. Tybulewicz.** 2010. The SYK tyrosine kinase: a crucial player in diverse biological functions. Nat. Rev. Immunol. **10:**387–402.
28. **Moriguchi, T., et al.** 2005. WNK1 regulates phosphorylation of cation-chloride-coupled cotransporters via the STE20-related kinases, SPAK and OSR1. J. Biol. Chem. **280:**42685–42693.
29. **Murthy, M., G. Cope, and K. M. O'Shaughnessy.** 2008. The acidic motif of WNK4 is crucial for its interaction with the K channel ROMK. Biochem. Biophys. Res. Commun. **375:**651–654.
30. **Ohta, A., et al.** 2009. Targeted disruption of the Wnk4 gene decreases phosphorylation of Na-Cl cotransporter, increases Na excretion and lowers blood pressure. Hum. Mol. Genet. **18:**3978–3986.
31. **Pacheco-Alvarez, D., et al.** 2006. The Na+:Cl cotransporter is activated and phosphorylated at the amino-terminal domain upon intracellular chloride depletion. J. Biol. Chem. **281:**28755–28763.
32. **Richardson, C., and D. R. Alessi.** 2008. The regulation of salt transport and blood pressure by the WNK-SPAK/OSR1 signalling pathway. J. Cell Sci. **121:**3293–3304.
33. **Richardson, C., et al.** 2008. Activation of the thiazide-sensitive Na+-Cl- cotransporter by the WNK-regulated kinases SPAK and OSR1. J. Cell Sci. **121:**675–684.
34. **Ring, A. M., et al.** 2007. WNK4 regulates activity of the epithelial Na+ channel in vitro and in vivo. Proc. Natl. Acad. Sci. U. S. A. **104:**4020–4024.
35. **Ring, A. M., et al.** 2007. WNK4 regulates Na+ channel and K+ channel activity and has implications for aldosterone signaling and K+ homeostasis. Proc. Natl. Acad. Sci. U. S. A. **104:**4025–4029.
36. **Sanderson, M. P., C. W. Lau, A. Schnapp, and C. W. Chow.** 2009. Syk: a novel target for treatment of inflammation in lung disease. Inflamm. Allergy Drug Targets **8:**87–95.
37. **Subramanya, A. R., J. Liu, D. H. Ellison, J. B. Wade, and P. A. Welling.** 2009. WNK4 diverts the thiazide-sensitive NaCl cotransporter to the lysosome and stimulates AP-3 interaction. J. Biol. Chem. **284:**18471–18490.
38. **Tabcharani, J. A., X. B. Chang, J. R. Riordan, and J. W. Hanrahan.** 1991. Phosphorylation-regulated Cl- channel in CHO cells stably expressing the cystic fibrosis gene. Nature **352:**628–631.
39. **Tang, W., and M. J. Wildey.** 2004. Development of a colorimetric method for functional chloride channel assay. J. Biomol. Screen. **9:**607–613.
40. **Ulanova, M., F. Duta, L. Puttagunta, A. D. Schreiber, and A. D. Befus.** 2005. Spleen tyrosine kinase (Syk) as a novel target for allergic asthma and rhinitis. Expert Opin. Ther. Targets **9:**901–921.
41. **Ulanova, M., et al.** 2006. Involvement of Syk kinase in TNF-induced nitric oxide production by airway epithelial cells. Biochem. Biophys. Res. Commun. **351:**431–437.
42. **Ulanova, M., et al.** 2005. Syk tyrosine kinase participates in beta1-integrin signaling and inflammatory responses in airway epithelial cells. Am. J. Physiol. Lung Cell. Mol. Physiol. **288:**L497–L507.
43. **Veríssimo, F., and P. Jordan.** 2001. WNK kinases, a novel protein kinase subfamily in multi-cellular organisms. Oncogene **20:**5562–5569.
44. **Vitari, A. C., M. Deak, N. A. Morrice, and D. R. Alessi.** 2005. The WNK1 and WNK4 protein kinases that are mutated in Gordon's hypertension syndrome phosphorylate and activate SPAK and OSR1 protein kinases. Biochem. J. **391:**17–24.
45. **Wilson, F. H., et al.** 2001. Human hypertension caused by mutations in WNK kinases. Science **293:**1107–1112.
46. **Wilson, F. H., et al.** 2003. Molecular pathogenesis of inherited hypertension with hyperkalemia: the Na-Cl cotransporter is inhibited by wild-type but not mutant WNK4. Proc. Natl. Acad. Sci. U. S. A. **100:**680–684.
47. **Yang, C. L., J. Angell, R. Mitchell, and D. H. Ellison.** 2003. WNK kinases regulate thiazide-sensitive Na-Cl cotransport. J. Clin. Invest. **111:**1039–1045.
48. **Yang, C. L., et al.** 2007. WNK1 and WNK4 modulate CFTR activity. Biochem. Biophys. Res. Commun. **353:**535–540.
49. **Yang, C. L., X. Zhu, Z. Wang, A. R. Subramanya, and D. H. Ellison.** 2005. Mechanisms of WNK1 and WNK4 interaction in the regulation of thiazide-sensitive NaCl cotransport. J. Clin. Invest. **115:**1379–1387.
50. **Yang, S. S., et al.** 2007. Molecular pathogenesis of pseudohypoaldosteronism type II: generation and analysis of a Wnk4(D561A/+) knockin mouse model. Cell Metab. **5:**331–344.
51. **Zheng, W., et al.** 2009. Hypoxia inducible factor-1 (HIF-1)-mediated repression of cystic fibrosis transmembrane conductance regulator (CFTR) in the intestinal epithelium. FASEB J. **23:**204–213.
52. **Zhou, B., et al.** 2010. WNK4 enhances the degradation of NCC through a sortilin-mediated lysosomal pathway. J. Am. Soc. Nephrol. **21:**82–92.